

Structure-function relationship of CAP-Gly domains

Anke Weisbrich^{1,4}, Srinivas Honnappa^{1,4}, Rolf Jaussi¹, Oksana Okhrimenko², Daniel Frey¹, Ilian Jelesarov², Anna Akhmanova³ & Michel O Steinmetz¹

In all eukaryotes, CAP-Gly proteins control important cellular processes. The molecular mechanisms underlying the functions of CAP-Gly domains, however, are still poorly understood. Here we use the complex formed between the CAP-Gly domain of p150^{glued} and the C-terminal zinc knuckle of CLIP170 as a model system to explore the structure-function relationship of CAP-Gly-mediated protein interactions. We demonstrate that the conserved GKNDG motif of CAP-Gly domains is responsible for targeting to the C-terminal EEY/F sequence motifs of CLIP170, EB proteins and microtubules. The CAP-Gly-EEY/F interaction is essential for the recruitment of the dynactin complex by CLIP170 and for activation of CLIP170. Our findings define the molecular basis of CAP-Gly domain function, including the tubulin detyrosination-tyrosination cycle. They further establish fundamental roles for the interaction between CAP-Gly proteins and C-terminal EEY/F sequence motifs in regulating complex and dynamic cellular processes.

The cytoskeleton-associated protein-glycine-rich domain (CAP-Gly; Pfam accession code PF01302) is a small, approximately 80-residue protein module¹ conserved in organisms from yeast to human. CAP-Gly domains have central functions in many proteins, including cytoplasmic linker proteins (CLIPs and CLIPRs), the large subunit of the dynactin complex (DCTN1, or p150^{glued}), tubulin folding cofactors B and E, centrosome-associated protein-350 (CAP350), the kinesin protein KIF13b and the familial cylindromatosis tumor suppressor CYLD. These proteins are implicated in essential cellular processes such as chromosome segregation, establishment and maintenance of cell polarity, intracellular organelle and vesicle transport, cell migration, intracellular signaling and oncogenesis (reviewed in refs. 2–9).

The CAP-Gly motif is generally considered to function as a tubulin-binding module, and most recently CAP-Gly domains of microtubule plus end-binding proteins (+TIPs) have been implicated in the tubulin detyrosination-tyrosination cycle^{10–13}. Although high-resolution structures of both the characteristic CAP-Gly fold and a complex between p150^{glued} and end-binding protein 1 (EB1) have provided the first insights into the properties of CAP-Gly domains^{14–17}, the molecular basis of CAP-Gly-mediated protein-protein interactions remains poorly understood. One well-established interaction involving a CAP-Gly domain is between the N-terminal CAP-Gly domain of p150^{glued} and the C-terminal zinc knuckles of CLIP170 (refs. 18–20). The p150^{glued}-CLIP170 interaction links CLIP170 to the dynein-dynactin pathway and is essential for the efficient recruitment of dynactin to growing microtubule plus ends^{19,21,22}. The complex is also implicated in chromosome alignment during mitosis²³. Notably, a G59S mutation in the CAP-Gly domain of p150^{glued} is linked to an

autosomal-dominant form of a motor neuron disease in humans²⁴. It has been suggested that this CAP-Gly domain defect interferes with the function of dynactin in the dynein-mediated retrograde transport of vesicles and organelles along microtubules within axons, perhaps owing to a loss of CLIP170 and tubulin binding^{19,24,25}.

In the present study, we exploited the human p150^{glued}-CLIP170 complex as a model system to gain insight into CAP-Gly domain structure and function using X-ray crystallography, high-sensitivity isothermal titration calorimetry (ITC), fluorescence resonance energy transfer (FRET), fluorescence microscopy and directed mutagenesis. Using this system, we found that the conserved GKNDG motif of CAP-Gly domains is required for targeting CAP-Gly proteins to C-terminal EEY/F sequence motifs. Further, we show that this binding is essential both for recruitment of dynactin by CLIP170 in cells and for activating the autoinhibited state of CLIP170. Our findings establish the molecular basis for understanding the function of CAP-Gly domains in general.

RESULTS

Biophysical and structural analysis of p150n-ClipZn2

The minimum core of the p150^{glued}-CLIP170 complex has been mapped to the N-terminal CAP-Gly domain of p150^{glued}, denoted p150n, and the C-terminal domain of CLIP170, which harbors two tandem repeated zinc-knuckle motifs^{18,19}. To test the properties of p150n binding to the isolated zinc knuckles (ClipZn1 and ClipZn2) and tandem repeated zinc knuckles (ClipZn12), we performed ITC studies at 25 °C. No binding was observed between p150n and ClipZn1 (**Table 1**), in agreement with previous results^{18,19}. In contrast, ITC analysis of p150n-ClipZn2 yielded a binding isotherm that

¹Biomolecular Research, Structural Biology, Paul Scherrer Institut, CH-5232 Villigen PSI, Switzerland. ²Biochemisches Institut der Universität Zürich, Winterthurerstrasse 190, CH-8057 Zürich, Switzerland. ³Department of Cell Biology, Erasmus Medical Center, P.O. Box 2040, 3000 CA Rotterdam, The Netherlands. ⁴These authors contributed equally to this work. Correspondence should be addressed to M.O.S. (michel.steinmetz@psi.ch).

Received 20 March; accepted 12 July; published online 9 September 2007; doi:10.1038/nsmb1291

Table 1 Equilibrium dissociation constants obtained by ITC

Proteins	K_d (μ M)	Proteins	K_d (μ M)	Proteins	K_d (μ M)
p150n ClipZn12	1.5 \pm 0.1	p150n(Q93K) ClipZn2	0.40 \pm 0.1	p150n EB1c(Y268F)	2.4 \pm 0.1
p150n ClipZn1	n.b. ^a	p150n(Q93R) ClipZn2	0.38 \pm 0.1	p150n EB1c(Y268I)	31.8 \pm 0.9
p150n ClipZn2	2.3 \pm 0.4	p150n ClipZn2 Δ C	n.b. ^a	p150n EB1c(Y268G)	24.4 \pm 0.8
p150n(K68A) ClipZn2	137 \pm 50	p150n ClipZn2(I1410H)	19.0 \pm 0.8	ClipCG12 EB1c	4.9 \pm 0.1
p150n(N69A) ClipZn2	85 \pm 5	p150n ClipZn2(I1410D)	15.7 \pm 0.4	ClipCG1 EB1c	13.5 \pm 0.3
p150n(N69H) ClipZn2	11.4 \pm 0.3	p150n EB1c	2.4 \pm 0.2	ClipCG2 EB1c	29.7 \pm 1.0
p150n(K68A N69A) ClipZn2	> 1,000 ^b	p150n(N69A) EB1c	34.8 \pm 2.0	ClipCG1 ClipZn1	13.5 \pm 0.5
p150n(R90P) ClipZn2	300 \pm 50	p150n(N69H) EB1c	3.1 \pm 0.3	ClipCG1 ClipZn2	5.1 \pm 0.1
p150n(R90S) ClipZn2	>300	p150n(K68A N69A) EB1c	> 1,000 ^b	ClipCG2 ClipZn1	27.1 \pm 0.8
				ClipCG2 ClipZn2	9.7 \pm 0.2

Protein samples were prepared in 10 mM sodium phosphate (pH 7.4) and 150 mM NaCl. Buffers for experiments carried out with ClipZn fragments were supplemented with 5 mM β -mercaptoethanol and 0.1 mM $ZnCl_2$. All measurements were performed at 25 °C. The fitting errors are indicated for each K_d value; the standard error in repeated experiments was typically between 15% and 20%. The binding stoichiometries, n , are as follows: p150n–ClipZn, $n = 1 \pm 0.1$; p150n–EB1c(dimer), $n = 2 \pm 0.2$; ClipCG12–EB1c(dimer), $n = 1 \pm 0.1$; ClipCG–ClipZn, $n = 1 \pm 0.1$.

^aNo binding. ^bData could not be subjected to rigorous analysis; however, the shapes of the binding isotherms suggest that the K_d values are in the millimolar range.

suggests a stoichiometry for the complex of 1 mol p150n/1 mol ClipZn2 (Fig. 1a, left graph). The K_d of p150n–ClipZn2 was determined to be 2 μ M. A similar K_d value was obtained for p150n–ClipZn12 (Table 1). Static light-scattering experiments with p150n and ClipZn2 yielded average molecular masses of 10.6 and 5.7 kDa, respectively (data not shown), consistent with the calculated masses of the monomers (10.2 and 4.8 kDa, respectively). Analysis of equimolar mixtures of p150n and ClipZn2 yielded an average molecular mass of 14.1 kDa. This value suggests the formation of a complex with a molar p150n/ClipZn2 ratio of 1:1, consistent with the ITC analysis. Together, these data show that the second zinc knuckle of Clip170 is both necessary and sufficient for binding to the CAP-Gly domain of p150n^{glued} and that these two domains form a heterodimer in solution.

To further characterize the p150n–ClipZn2 complex, we determined its structure by X-ray crystallography to 2.6-Å resolution. The overall structure reveals a heterodimeric complex formed between one p150n and one ClipZn2 molecule (Fig. 1b), consistent with the solution data (see above). The asymmetric unit of the crystal contains four copies of the complex with nearly identical main chain and side chain conformations (r.m.s. deviation for all atoms equals 0.3 Å). The p150n subunit has all the features of the CAP-Gly fold^{14,15} and is very similar to its free, uncomplexed form (PDB 2HKN; r.m.s. deviation for all atoms equals 0.4 Å). The structure of the ClipZn2 subunit is composed of two short β -strands followed by a short loop and an extended C terminus. The main chain of the N-terminal moiety of ClipZn2 wraps around a metal ion that is coordinated by a CCHC side chain motif (Fig. 1b), an arrangement characteristic of zinc-finger domains found in retroviral nucleocapsid proteins²⁶. The presence of a zinc ion was confirmed using X-ray fluorescence scans of p150n–ClipZn2 crystals at the absorption edge of zinc (data not shown).

Analysis of the p150n–ClipZn2 binding interface reveals two distinct contact sites, A and B (Fig. 1c). Contact A involves residues from a distinct groove shaped by a number of hydrophobic and polar side chains of p150n and the last five C-terminal residues of ClipZn2 (Figs. 2 and 3). This short ClipZn2 sequence stretch, DDETF, assumes an extended conformation and packs against the β 6 strand of p150n in an antiparallel fashion. The Phe1427 side chain is inserted at one end of the p150n groove and packs against the side chains of Phe52, Trp57, Val73 and Phe88. Its terminal α -carboxylate group, COO⁻, forms hydrogen bonds with the N δ 2 side chain atom of Asn69 and the main chain NH of Phe88. An additional main chain–main chain hydrogen

bond is established between the NH of Phe1427 and the oxygen of Phe88. Lys68 and Val89 of p150n form hydrogen bonds and a hydrophobic contact to the side chain and main chain of ClipZn2 Thr1426. This interaction network is completed by additional contacts between Ser92 and Gln93 of p150n and Asp1423 of ClipZn2 (Fig. 2a,b). Deleting the last three C-terminal residues of ClipZn2 abolished binding of the mutant fragment, ClipZn2 Δ C, to p150n, demonstrating that the ClipZn2 tail is essential for complex formation (Fig. 1a, left graph, and Table 1).

Contact B involves residues from the β 2– β 3 and β 6– β 7 loops of p150n and the zinc-binding domain of ClipZn2 (residues 1406–1427; Fig. 1b,c). The guanidinium group of Arg90 of p150n forms an intramolecular arginine– π stacking interaction with Trp57; it is within van der Waals distance of the S_γ atom of ClipZn2 Cys1411, makes an intermolecular water-mediated hydrogen bonding contact to the main chain oxygen of Asn1422 and is in position to form a putative long-range attractive electrostatic interaction with the CCHC–zinc ion cluster. Furthermore, the aliphatic moiety of Arg90 packs against Ile1410 of ClipZn2. Additional contacts are formed between Thr54, Gly55, Lys56 and Gln91 of p150n, and Met1413 and Glu1412 of ClipZn2 (Fig. 2b,c).

Probing the p150n–ClipZn2 interaction by mutagenesis

Most contacting residues seen at the p150n–ClipZn2 complex interface are highly conserved in CAP-Gly domains of p150n^{glued} and in zinc knuckles of CLIP170 metazoan orthologs, suggesting that the p150n^{glued}–CLIP170 binding mode is well conserved across evolution (Fig. 2d,e). However, many of these residues are not conserved in unrelated CAP-Gly domain-containing proteins (Fig. 3a). On the basis of our alignments and structural information (Figs. 2 and 3), we chose to target specific conserved and variable residues for mutagenesis. The binding properties of the resulting variants were assessed by ITC, and the resulting K_d values are summarized in Table 1.

Mutation of either Lys68 and Asn69 within the GKNDG motif, which is highly conserved in many CAP-Gly domains¹⁴, to alanine (p150n(K68A) and p150n(N69A)) reduced the binding affinity of these p150n mutant proteins for ClipZn2 \sim 50-fold (Fig. 1a, right graph). The double mutation in p150n(K68A N69A) essentially abolished complex formation. These findings demonstrate the importance of the Lys–Asn dipeptide segment of the GKNDG motif in recognizing the C-terminal DDETF sequence of ClipZn2. Notably, mutating Asn69 to histidine (p150n(N69H)), as observed in the

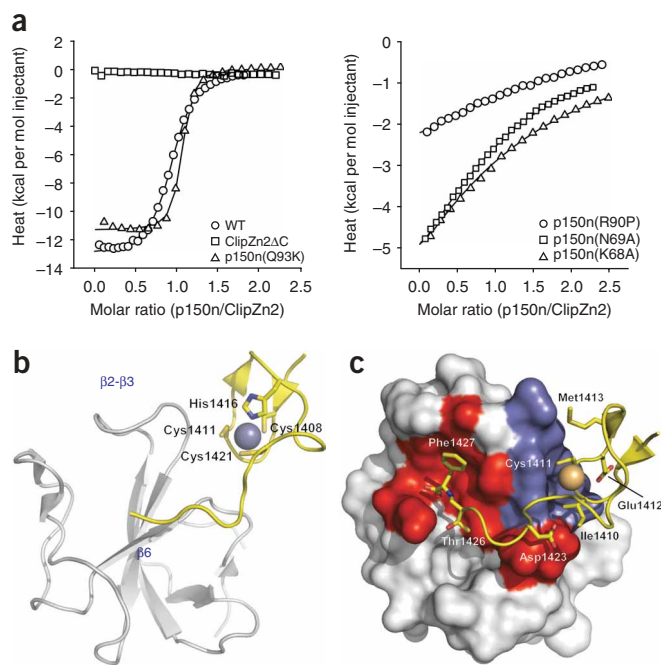


Figure 1 Binding studies and X-ray crystal structure of p150n-ClipZn2. (a) Binding isotherms obtained by ITC. Left, p150n-ClipZn2 (WT), p150n(Q93K)-ClipZn2 and p150n-ClipZn2ΔC. Right, p150n(R90P)-ClipZn2, p150n(K68A)-ClipZn2 and p150n(N69A)-ClipZn2. Solid lines are fits where we assumed one binding site. (b) Overall view of heterodimeric complex formed between p150n (residues Pro26–Phe97; light gray) and ClipZn2 (residues Pro1406–Phe1427; yellow) in cartoon representation. Secondary structure elements of p150n that contact ClipZn2 are indicated. The three cysteine and one histidine side chains that coordinate the zinc ion (blue sphere) in ClipZn2 are shown as sticks. (c) As in b but with surface representation of p150n. Red and blue, the two ClipZn2 contact sites, A and B, respectively. Side chains of ClipZn2 that contact p150n are shown as sticks.

CAP-Gly domains of CLIPR59 and α -tubulin chaperone cofactor E (Fig. 3a), did not alter the affinity of the p150n mutant. Consistent with this observation, modeling indicates that the hydrogen bonding of Asn69 to the COO⁻ group of ClipZn2 can also be established by a histidine side chain.

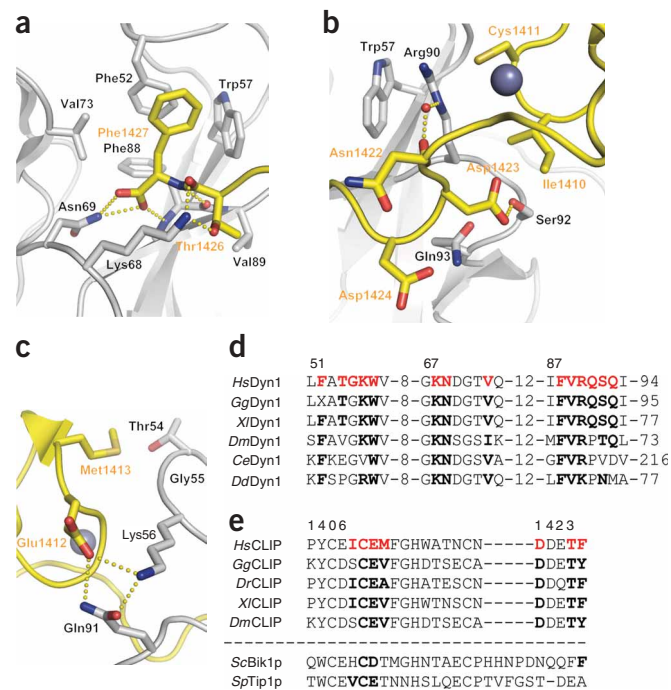
Gln93 of p150n, which contacts Asp1423 of DDETF, is not conserved in CAP-Gly domain homologs. Instead, the corresponding sequence position shows a strong preference for basic residues (Fig. 3a). Modeling suggests that a basic residue in p150n may favorably interact with Asp1423 or Asp1424 of ClipZn2, or both (Fig. 2b). In support of this prediction, we found that replacing Gln93 with either lysine (p150n(Q93K)) or arginine (p150n(Q93R)) increased the binding affinity of these p150n mutant proteins for ClipZn2 about six-fold (Fig. 1a, left graph). This finding suggests that the nature of the residue occupying position 93 modulates the affinity of CAP-Gly domains for C-terminal acidic-aromatic sequence motifs.

Figure 2 Binding interface of p150n-ClipZn2, and sequence conservation. (a–c) Close-up views of the interaction network in the p150n-ClipZn2 complex, in cartoon (main chains) and stick (contacting residues) representation. Light gray carbons, p150n; yellow carbons, ClipZn2. (d,e) Alignments of the sequence regions of p150n^{glued} (d) and CLIP170 (e) orthologs that form intermolecular contacts in p150n-ClipZn2. Bold red, residues that interact in our p150n-ClipZn2 structure; bold black, conservation of these residues. Human p150n^{glued} and CLIP170 position numbers are indicated above the alignments. In e, asterisks below alignment mark the four zinc-coordinating residues of ClipZn2, and dashed line separates metazoan proteins from their yeast orthologs, which substantially diverge in sequence. Last residue of each sequence in e corresponds to the C terminus. *Hs*, *Homo sapiens*; *Gg*, *Gallus gallus*; *Xl*, *Xenopus laevis*; *Dr*, *Dario rerio*; *Dm*, *Drosophila melanogaster*; *Ce*, *Caenorhabditis elegans*; *Dd*, *Dictyostelium discoideum*; *Sc*, *Saccharomyces cerevisiae*; *Sp*, *Saccharomyces pombe*. Sequence accession codes are as follows (UniProtKB/Swiss-Prot except where stated otherwise). Dyn1: *Hs*, Q14203; *Gg*, P35458; *Xl*, Q6PCJ1; *Dm*, P13496; *Ce*, NCBI Protein NP_506367; *Dd*, NCBI Protein EAL67196. CLIP: *Hs*, P30622; *Gg*, O42184; *Xl*, GenBank EST BJ620851; *Dr*, GenBank XM_694251; *Dm*, Q9VJE5. ScBik1p, P11709; SpTip1p, P79065.

Arg90, which is highly conserved in p150^{glued} orthologs, seems to be important for ClipZn2 zinc-knuckle binding. However, the residue is not well conserved in CAP-Gly domain homologs; some CLIPs contain a proline or a serine at the corresponding position (Fig. 3a). Replacing Arg90 with these residues resulted in a >100-fold reduction in binding affinity of the mutant p150n proteins, p150n(R90P) and p150n(R90S), for ClipZn2 (Fig. 1a, right graph). Substituting histidine or aspartate for the conserved Ile1410 of ClipZn2 contacted by Arg90 (Fig. 2b) reduced binding affinity of the mutant domains, ClipZn2(I1410H) and ClipZn2(I1410D), for p150n about ten-fold. These findings underscore the key role of p150n Arg90 in binding the zinc-knuckle moiety of ClipZn2. An arginine residue at position 90 has also been found to be important for the interaction between p150n and the acidic C-terminal tail of EB1, denoted EB1c^{16,17}.

Functional analysis of the p150n-ClipZn2 interaction

Previous work has shown the importance of the CLIP170 zinc-knuckle domain for recruitment of endogenous dynactin to CLIP170-decorated microtubules or microtubule tips^{18,19}. Such recruitment can be readily observed in CLIP170-overexpressing cells, in which dynactin relocates to CLIP170-induced microtubule bundles



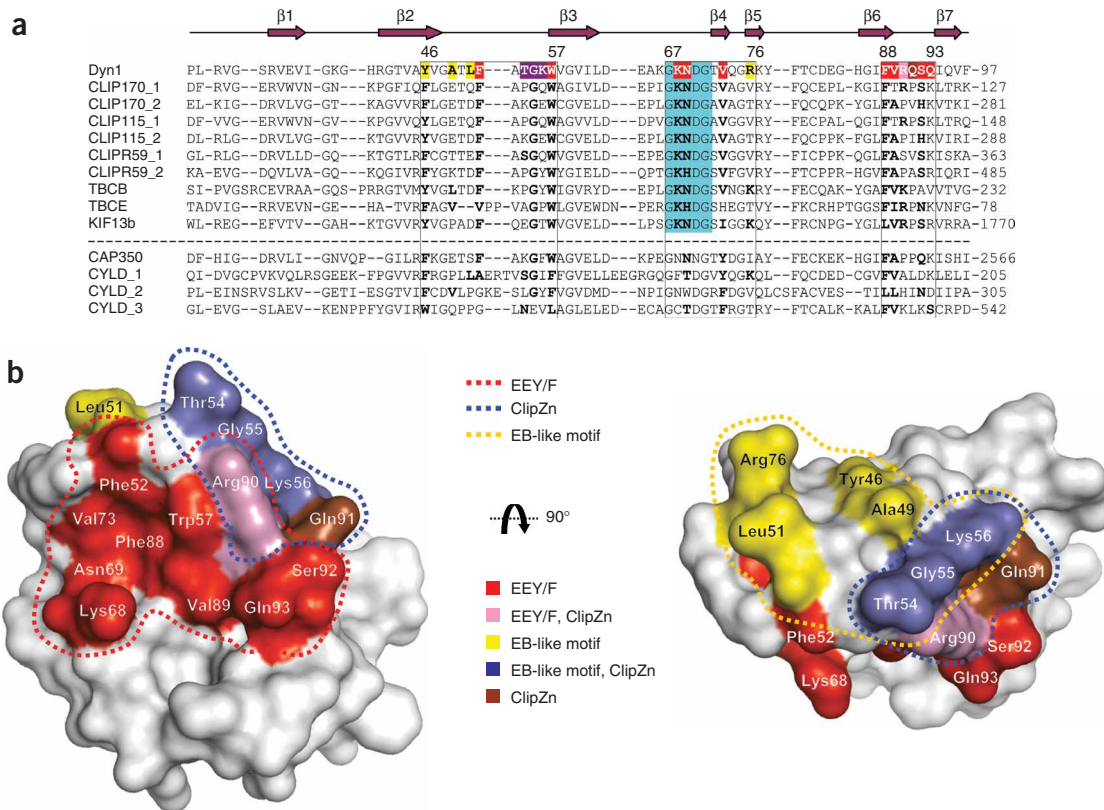


Figure 3 Sequence conservation and binding sites of CAP-Gly domain homologs. **(a)** Structure-based sequence alignment of human CAP-Gly domain homologs. p150^{glued} residues engaged in protein-protein interactions are grouped into three sequence areas (boxed) and colored by interaction partner (see key in **b**). Bold, conservation in other CAP-Gly domains; turquoise, GKNDG motif, which is highly conserved in many CAP-Gly domains; dashed line separates CAP-Gly domains with an intact GKNDG motif from those with sequence changes in this region. Secondary structure elements and p150^{glued} residue numbering are indicated above the alignment. UniProtKB/Swiss-Prot sequence accession numbers are as follows: Dyn1, Q14203; CLIP170, P30622; CLIP115, Q9UDT6; CLIPR59, Q96DZ5; TBCB, Q99426; TBCE, Q15813; KIF13b, Q9NQT8; CAP350, Q5VT06; CYLD, Q9NQC7. **(b)** Two views of p150n in surface representation. Interacting residues are grouped in three partially overlapping regions indicated by dashed lines (red, EEY/F binding regions; blue, CLIP zinc knuckle binding; yellow, EB-like motif binding).

(Fig. 4a,b). Our structural and biophysical studies predict that the C-terminal DDETF sequence segment of CLIP170 is important in dynactin recruitment. To test this hypothesis, we attached a cyan fluorescent protein (CFP) tag to the C terminus of CLIP170, reasoning that this bulky protein moiety should interfere with the interaction of the DDETF tail with the CAP-Gly domain of p150^{glued}. Indeed, placement of a CFP tag at the extreme C terminus of CLIP170 completely blocked dynactin recruitment to CLIP170-associated bundles (Fig. 4c). In contrast, when the CFP tag was inserted upstream of the zinc-knuckle domains, so that the DDETF tail was not occluded, robust binding of dynactin to CLIP170-induced microtubule bundles was observed (Fig. 4d). Deletion of the DDETF sequence also abolished dynactin association with the CLIP170-bundled microtubules (Fig. 4e). Together, these data suggest that the C-terminal DDETF sequence segment is important for CLIP170-mediated dynactin localization in cells.

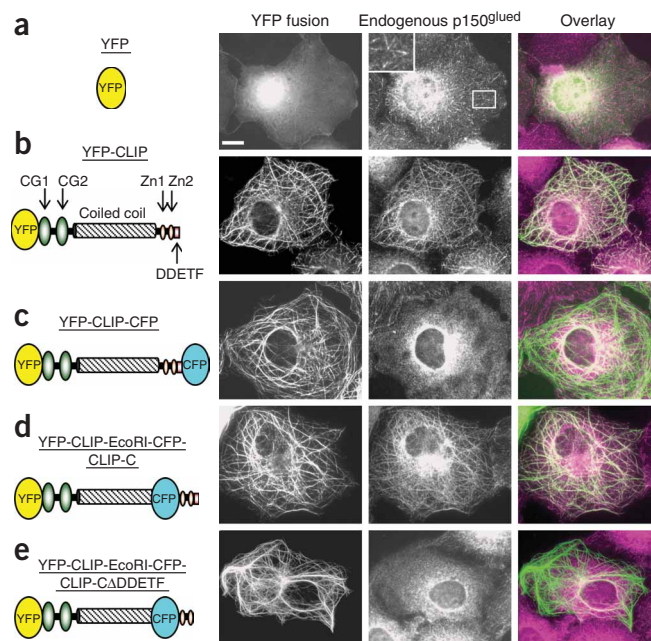
CAP-Gly domain binding to C-terminal EEY/F sequence motifs

Our studies demonstrate that binding of the C-terminal DDETF tail of CLIP170 to the CAP-Gly domain of p150^{glued} is crucial for the p150^{glued}-CLIP170 interaction (see above). The distinct DDETF-binding groove of p150n encompassing the GKNDG motif of the β 3- β 4 loop is highly conserved among CAP-Gly domain homologs

and corresponding orthologs from otherwise unrelated proteins (Fig. 3a), supporting the idea of functional selection. We have shown previously that a similar acidic peptide derived from the C terminus of EB1, EQEEY, binds the same highly conserved groove of p150n¹⁷. As for ClipZn2, this sequence segment of EB1 is crucial for stable complex formation with p150n^{16,17}. Remarkably, the modes of binding between the EB1 and CLIP170 C-terminal peptide segments and p150n are very similar (Fig. 5a). Along the same lines, recent studies have demonstrated that the tyrosine in the C-terminal EGEEY sequence of α -tubulin is a major factor affecting the recruitment of CAP-Gly proteins to microtubule plus ends^{10,12,13,17}. Together, these findings demonstrate that C-terminal acidic-aromatic sequence motifs, referred to as EEY/F from here on, are signals in the sequences of CLIP170, EB proteins and microtubules (Fig. 5b) that specifically target CAP-Gly proteins.

To test the importance of the Lys-Asn dipeptide segment of the GKNDG motif for the interaction of p150n with the dimeric EB1c domain²⁷, we performed ITC binding studies with wild-type and mutant proteins. Analysis of the binding isotherm revealed a stoichiometry for the complex of 2 mol p150n/1 mol EB1c dimer (Fig. 5c, left graph), consistent with previous findings¹⁷. The K_d of p150n-EB1c was determined to be 3 μ M (Table 1). An approximately ten-fold lower affinity was observed for p150n(N69A), whereas p150n(N69H)

Figure 4 The C-terminal DDEF sequence segment of CLIP170 is required for dynein recruitment to CLIP170-associated microtubules. (a–e) COS-7 cells were transfected with constructs expressing YFP or the indicated fluorescent CLIP170 fusions and stained for endogenous p150^{glued}. Schematic representations of CLIP170 fusions are shown at left; CAP-Gly domains (CG1, CG2), zinc knuckles (Zn1, Zn2), DDEF motif and coiled-coil region are indicated. Right images show overlays of YFP fluorescence (green) and staining of endogenous p150^{glued} (magenta). Inset in the middle panel in **a** shows an enlargement of the boxed area to illustrate localization of p150^{glued} to microtubule tips in control cells. Bar, 10 μ m.



showed a K_d very similar to that of wild-type p150n. Binding of the double mutant p150n(K68A N69A) to EB1c was essentially abrogated. The relative changes in affinities obtained for the mutant p150n–EB1c complexes were very similar to those found for p150n–ClipZn2 (see above).

We used mutagenesis to further examine the role of the EB1c terminal tyrosine residue's side chain in the p150n–EB1c interaction. As expected from the structural data (Fig. 2a and Fig. 5a), mutating Tyr268 to phenylalanine did not substantially change the affinity of the mutant EB1c protein, EB1c(Y268F), for p150n, demonstrating that the OH group of this tyrosine side chain has no role in binding (Fig. 5c, right graph, and Table 1). In contrast, an isoleucine or glycine at position 268 reduced the affinity of the mutant EB1c proteins, EB1c(Y268I) and EB1c(Y268G), for p150n about ten-fold, indicating that the aromatic ring of tyrosine or phenylalanine is crucial for the interaction with the highly conserved hydrophobic groove of CAP-Gly domains.

Finally, we analyzed binding between EB1c and the CAP-Gly domains of CLIP170, denoted ClipCG1 and ClipCG2 for the individual and ClipCG12 for the tandem repeated CAP-Gly domain fragments. ITC binding isotherms suggest a stoichiometry for the complex of 1 mol EB1c dimer/1 mol ClipCG12 monomer and yield a K_d of 5 μ M (Table 1). Approximately three- and six-fold weaker binding was observed for ClipCG1 and ClipCG2, respectively, which each bound with a stoichiometry of 1 mol EB1c dimers/2 mol CAP-Gly domain monomers. The weaker affinity of both the ClipCG constructs for EB1c, compared to that of p150n, can be explained by the residue composition of the β 2– β 3 loop of the CAP-Gly domains (Fig. 3). This loop, and in particular the residue at the second position in the loop (Glu79 and Glu233 in CLIP170 and Ala49 in p150^{glued}), are crucial elements for interacting with the highly conserved hydrophobic groove of the EB-like motif of EB1c¹⁷. Modeling and mutagenesis have shown that a glutamate at the second position of the β 2– β 3 loop destabilizes the interaction between CAP-Gly and EB-like motifs¹⁷.

In summary, these findings, together with the mutagenesis analysis of p150n–ClipZn2, establish that CAP-Gly domains harboring an intact GKNDG sequence are specific recognition domains for EEY/F motifs. As will be further elaborated and discussed below, the CAP-Gly–EEY/F interaction regulates a wide range of important microtubule-based processes in all eukaryotic organisms and thus is fundamental for controlling microtubule function.

The role of CAP-Gly–EEY/F interactions in CLIP170 activation

Previous studies have shown that CLIP170 exists in an active ‘open’ or an autoinhibited ‘closed’, folded-back state, which are controlled by the interaction of its N terminus, containing the two CAP-Gly domains, with the C-terminal zinc knuckles^{18,19}. To test the binding of the two isolated CAP-Gly domains of CLIP170 to the two zinc knuckle-containing fragments ClipZn1 and ClipZn2, we performed ITC binding studies. ClipCG1 and ClipCG2 show K_d values for

binding to ClipZn2 of 5 and 10 μ M, respectively (Fig. 6a and Table 1). The binding isotherms suggest a stoichiometry for the complexes of 1 mol CAP-Gly domain/1 mol ClipZn2. Approximately three-fold lower binding affinity was observed for ClipZn1. Notably, under the particular *in vitro* conditions we used, the complexes formed with either ClipZn1 or ClipZn2 can be distinguished by their reaction enthalpies and entropies (Supplementary Table 1 online). Together, these data suggest that both CAP-Gly domains preferentially interact with the second zinc knuckle. However, the observation that all four K_d values are between 5 and 27 μ M indicates that they discriminate moderately between the two C-terminal zinc knuckles of CLIP170. This finding contrasts with the binding properties of the CAP-Gly domain of p150^{glued}, which is highly specific for the second zinc knuckle of CLIP170 (see above and Table 1).

To test the role of CAP-Gly–EEY/F interactions in CLIP170 activation, we measured FRET in cell extracts. This assay has been used successfully before to show head-to-tail interaction in CLIP170 (ref. 19). To probe the function of the C-terminal DDEF sequence of CLIP170, we inserted the CFP in front of the first zinc knuckle (Fig. 4d). Two slightly different versions of this ‘internal’ CLIP170 FRET sensor were used, with CFP inserted either 80 or 129 amino acid residues upstream of the CLIP170 C terminus, denoted YFP-CLIP-BamHI-CFP-CLIP-C and YFP-CLIP-EcoRI-CFP-CLIP-C, respectively. The fluorescence of the yellow fluorescent protein (YFP) donor after excitation of the CFP acceptor was the same for the two internal CLIP170 FRET sensors. Deletion of the last five residues of CLIP170 reduced the FRET signal in both sensors (Fig. 6b and data not shown). Additional mutation of the first two cysteines of the CCHC motif in the first zinc knuckle to serines (SSHC) completely abolished FRET, in agreement with previous observations¹⁹. Notably, the FRET efficiency observed for the original YFP-CLIP-CFP fusion (Fig. 4c), in which the C-terminal DDEF is blocked by CFP, was similar to those of the nonmutated internal FRET sensors (data not shown), indicating that the unblocked C terminus is not essential for CLIP170 self-inhibition. This finding is in agreement with the ITC data revealing that the two CAP-Gly domains of CLIP170 bind both zinc knuckles with similar affinities (see above).

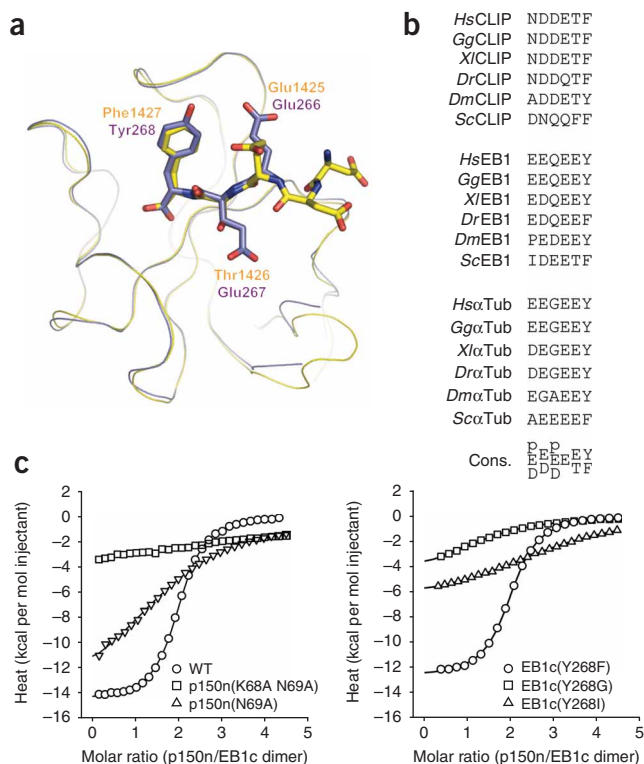


Figure 5 CAP-Gly domains as EEY/F motif-recognition domains.

(a) Superposition of p150n-ClipZn2 (yellow) with p150n-EB1c (magenta; PDB 2HKQ). Ribbons, CAP-Gly domains. Sticks, C-terminal sequence segments of binding partners. (b) Sequence alignment of C-terminal sequences of CLIP170, EB and α -tubulin proteins (species abbreviations as in Fig. 2d,e). Consensus sequence is shown below (Cons.; p denotes polar residues). (c) Binding isotherms of p150n-EB1c obtained by ITC. Left, p150n-EB1c (WT), p150n(N69A)-EB1c and p150n(K68A N69A)-EB1c. Right, p150n-EB1c(Y268F), p150n-EB1c(Y268I) and p150n-EB1c(Y268G). Solid lines are fits where we assumed two equivalent, noninteracting binding sites for p150n monomers on the EB1c dimer.

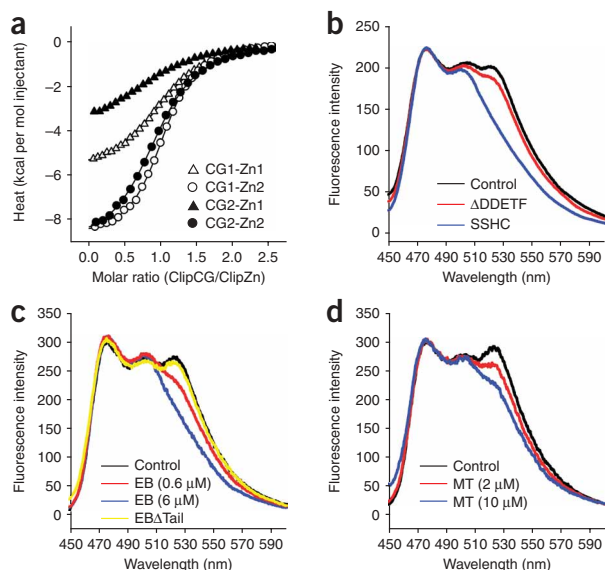
To test whether activation of CLIP170 could be induced by targeting either the CAP-Gly domains or the second zinc knuckle, including the DDETF sequence segment, we measured FRET with CLIP170 binding partners. Recombinant p150n had no effect on the FRET signal of YFP-CLIP-BamHI-CFP-CLIP-C or YFP-CLIP-EcoRI-CFP-CLIP-C (data not shown). This finding is consistent with p150n binding only to the second zinc knuckle (Table 1), whereas the first knuckle is more important for full-length CLIP170 self-association^{18,19}. In contrast, YFP emission of the CLIP170 FRET sensors after CFP excitation was affected by EB1c in a dose-dependent manner (Fig. 6c). This result can be explained by the presence of the C-terminal EQEEY sequence segment of EB1c, which targets the highly conserved hydrophobic groove encompassing the GKNDG motif of CAP-Gly domains (see above). In agreement with this conclusion, a mutant lacking the C-terminal 20 residues of EB1c (EB1c Δ Tail) did not relieve the autoinhibition of CLIP170 (Fig. 6c). Similar to the results with EB1c, the addition of taxol-stabilized microtubules also led to a lower CLIP170 FRET signal (Fig. 6d),

Figure 6 Activation of CLIP170. (a) Binding isotherms obtained by ITC for ClipCG1-ClipZn1, ClipCG1-ClipZn2, ClipCG2-ClipZn1 and ClipCG2-ClipZn2. Solid lines are fits where we assumed one binding site. (b) Emission spectra of YFP-CLIP-EcoRI-CFP-CLIP-C (control), YFP-CLIP-EcoRI-CFP-CLIP-CADDETF and YFP-CLIP-EcoRI-CFP-CLIP-CADDETF in which the first two cysteines of the CCHC motif of the first zinc knuckle were mutated to serines (SSHHC). (c) Emission spectra of cell extracts transfected with YFP-CLIP-BamHI-CFP-CLIP-C (control), after addition of 0.6 and 6 μ M (dimer equivalents) EB1c, respectively, and after addition of 8 μ M EB1c Δ Tail. Spectra were measured in PBS. (d) Emission spectra of cell extracts transfected with YFP-CLIP-BamHI-CFP-CLIP-C (control) and after addition of 2 and 10 μ M α / β -tubulin polymerized into microtubules (MT), respectively. Spectra were measured in PME buffer. Fluorescence intensities are plotted in arbitrary units. Spectra were obtained with excitation at 425 nm.

most probably owing to the presence of the EGEEY sequence segment of α -tubulin. Together, these findings demonstrate the importance of the CAP-Gly-EEY/F interaction for activation of the autoinhibited state of CLIP170 and indicate that, in cells, both EB proteins and tubulin can activate CLIP170.

DISCUSSION

Despite the important role of CAP-Gly proteins in central biological processes in all eukaryotes, the structure-function relationships of CAP-Gly domains are still poorly understood. In this study, we have used the CAP-Gly domain of p150^{glued} and the C-terminal zinc knuckle of CLIP170 as a model system to explore in detail the molecular basis of CAP-Gly domain-mediated protein interactions. Our data reveal that the binding of p150n to ClipZn2 is bipartite, involving a highly conserved primary site and a second protein target-specific site of the CAP-Gly fold. A bipartite binding mode has also been found previously for a complex formed between p150n and EB1c¹⁷. Notably, the EEY/F motifs of both ClipZn2 and EB1c interact, in similar binding modes, with the highly conserved groove of p150n encompassing the GKNDG sequence (Fig. 3 and Fig. 5a). The second, less conserved site on p150n that interacts with the zinc knuckle of ClipZn2 overlaps partially with the site that contacts the EB-like motif of EB1c. The finding that p150^{glued}-CLIP170, p150^{glued}-EB1 and CLIP170-EB1 use a common binding mechanism explains *in vivo* data suggesting that these interactions are mutually exclusive and compete with one another^{20,28}.



Our sequence analyses, quantitative binding studies and mutagenesis data systematically demonstrate that the precise residue compositions of both highly conserved and protein-specific sites positively and negatively modulate the affinity of CAP-Gly domains for their targets. This finding suggests that CAP-Gly domains have evolved as stable molecular scaffolds onto which evolution has grafted different binding functions and affinities as required in a given biological context. Notably, the Lys-Asn dipeptide segment of the GKNDG motif is completely or partially mutated in the CAP-Gly domains of CYLD and CAP350, respectively (Fig. 3a). Because this short sequence stretch is important for binding to C-terminal EEY/F motifs, we predict that the CAP-Gly domains of these proteins have low affinities for EEY/F sequence tails, such as those of CLIP170, EB proteins and α -tubulin. Indeed, the third CAP-Gly domain of CYLD binds NEMO (also called IKK γ) via a proline-rich sequence motif¹⁵, and a C-terminal CAP350 fragment encompassing the CAP-Gly domain has been found not to interact with EB1 and α -tubulin in yeast two-hybrid screens²⁹. Along the same lines, the origin of a variant of hypoparathyroidism-retardation-dysmorphism (HRD) syndrome has been linked to a 4-residue deletion immediately after the GKNDG motif of α -tubulin chaperone cofactor E³⁰. This mutation is expected to interfere with binding of the mutant CAP-Gly domain to the EEY/F tail of α -tubulin and thus may be the origin of the observed microtubule perturbations in disease cells³⁰.

The p150n-ClipZn2, p150n-EB1c and EB1c-ClipCG12 complexes have K_d values in the low micromolar range (Table 1). Comparable affinities have also been described for the interaction of CLIP and EB proteins with microtubules^{19,31,32}. As the CAP-Gly domains of p150^{glued} and CLIP170 are implicated in highly dynamic and regulated biological processes such as tracking of growing microtubule ends and dynein-dynactin motor movement^{19,31,33–38}, moderate-affinity interactions make sense. They are well suited to be broken and reformed quickly in response to movements of their target molecules. The multiple and partly competing interaction modes of the CAP-Gly domain and EEY/F proteins seem to be ideal for the recruitment and clustering of different molecular functions at a common location, such as the growing microtubule end. These considerations suggest that numerous low-affinity, modular binding sites in different combinations control the dynamics and remodeling of +TIP networks and probably form the basis of their plus end-tracking behavior.

A central finding of our study is that CAP-Gly domains harboring an intact GKNDG sequence specifically recognize EEY/F sequence motifs that are characteristic of CLIP170, EB and α -tubulin proteins (schematically illustrated in Fig. 7). The interaction between CAP-Gly and EEY/F protein tails regulates a wide range of important microtubule-based processes in all eukaryotic organisms and thus is fundamental for controlling microtubule function. For example, the interaction is essential for the recruitment of p150^{glued} by CLIP170 to growing microtubule plus ends, linking CLIP170 to the dynein-dynein pathway and contributing to cell motility and spindle positioning^{19,21–23}. In this context, it is noteworthy that, in humans, a missense G59S point mutation in the CAP-Gly domain of p150^{glued} has been implicated in an autosomal-dominant form of a motor neuron disease²⁴. This residue change is predicted to impair proper folding of the CAP-Gly domain of p150^{glued}, consistent with the observed aggregation of the mutant protein both *in vitro* and in cells²⁵. This p150^{glued} defect seems to perturb the function of dynactin in the dynein-mediated retrograde transport of vesicles and organelles along microtubules, most probably owing to loss of microtubule and CLIP170 binding at the EEY/F sequence tail^{19,24,25}. Loss of dynactin

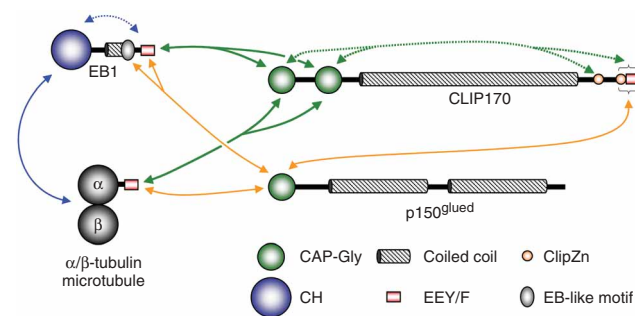


Figure 7 Schematic illustration of the protein-protein interaction network analyzed and discussed in the present study. Olive, orange and blue double arrows represent interactions mediated by CLIP170 CAP-Gly, p150^{glued} CAP-Gly and the calponin-homology (CH) domain of EB1, respectively. Dashed and solid lines denote intra- and intermolecular interactions, respectively. Note that EB1, CLIP170 and p150^{glued} form parallel dimers; however, for simplicity only the monomers are depicted.

function resulting from the G59S mutation is ultimately linked to motor-neuron cell death²⁵.

In addition, the interaction of the two C-terminal zinc knuckles of CLIP170 with its N-terminal CAP-Gly domains is responsible for the closed, autoinhibited conformation of the molecule (Fig. 7). Whereas the interaction with p150^{glued} relies on the second zinc knuckle, including the EEY/F sequence motif of CLIP170, autoinhibition more crucially depends on the first zinc-binding motif (Fig. 4; see also refs. 18,19). The individual CAP-Gly domains of CLIP170 bind the two zinc knuckles with similar low-micromolar affinities (Table 1). Thus, explanations of the greater importance of the first zinc-binding domain for the head-to-tail interaction should be sought in the context of the full-length CLIP170 molecule. Our data indicate, however, that CLIP170 self-inhibition involves a complex interplay of interactions between the CAP-Gly domains, the zinc knuckles and the C-terminal EEY/F motif. Notably, we found that exogenous EB1c and microtubules can relieve autoinhibition of CLIP170 in cell extracts (Fig. 6c,d). Both EB proteins and α -tubulin contain an EEY/F sequence motif (Fig. 5b). Our data suggest that the C-terminal tails of EB1 and α -tubulin can activate CLIP170 by targeting both CAP-Gly domains (see also the accompanying study in this issue³⁹). These observations indicate that the association of CLIP170 with microtubule plus ends, either directly or indirectly through EB proteins, may induce opening up of CLIP170 and release its C-terminal domain to interact with cargo molecules such as the dynein-dynactin motor complex. We did not observe activation of CLIP170 by the monomeric p150n fragment; however, this may well be triggered by the dimeric full-length p150^{glued} molecule³⁹. Activation of +TIPs through their associations with other members of this protein family represents a common theme in their function: the CAP-Gly domain of p150^{glued} activates EB1 by binding the EB1 EEY/F sequence motif, as well^{16,17}.

Finally, our findings provide a molecular explanation for the observation that a specialized subset of stable detyrosinated microtubules accumulate markedly fewer CAP-Gly proteins at their plus ends^{10–13}. In most eukaryotic cells, the EEY/F tail of α -tubulin is subjected to an enzymatic detyrosination-tyrosination cycle in which the C-terminal tyrosine is repeatedly cleaved and added back (reviewed in ref. 40). Suppression of this cycle leads to defects in spindle positioning, abnormal cell morphology, disorganized neuronal networks and tumor progression, underscoring the importance of this post-translational modification^{10–13}. Only very recently, α -tubulin tyrosination has been linked to the ability of the microtubule end to

recruit p150^{glued}, CLIP170 and CLIP115 (ref. 13), consistent with our conclusion that most CAP-Gly domains specifically recognize C-terminal EEY/F sequence motifs (Fig. 7). Thus, our findings also provide a molecular basis for understanding the fundamental role of the tubulin detyrosination-tyrosination cycle in controlling CAP-Gly proteins such as the CLIPs and the dynein–dynactin motor complex, and its consequences for microtubule function.

METHODS

Cloning, mutagenesis and protein preparation. The insertion of p150n (residues Met18–Ser111 of human p150^{glued}), EB1c (Asp191–Tyr268 of human EB1) and EB1cΔTail (Asp191–Ala248) in pET15b (Invitrogen) has been described¹⁷. ClipZn12 (residues Gly1395–Phe1427 of human CLIP170; numbering according to UniProtKB/Swiss-Prot entry P30622), ClipZn1 (Glu1357–Glu1404), ClipZn2 (Met1388–Phe1427), ClipCG12 (Ser48–Met300), ClipCG1 (Asp56–Val128) and ClipCG2 (Arg210–Gly282) were PCR-amplified from a human *CLIP170* complementary DNA clone⁴¹. The PCR products were subcloned by Gateway BP reactions into pDONR221 and thereafter by LR reactions into pETG20A-MTA according to the manufacturer's instructions (Invitrogen). All constructs permitted expression in *Escherichia coli* of N-terminal fusion proteins with thrombin-cleavable His₆-tags (pET15b expression constructs) or thioredoxin-His₆-tags (pETG20A-MTA expression constructs). CLIP170 constructs used for the fluorescence cell imaging and FRET experiments were cloned as described^{19,42}.

Mutagenesis was carried out using the corresponding plasmids as templates, as follows. 5'-phosphorylated primers were incorporated into circular DNA using Phusion DNA polymerase and Tsc ligase. The template plasmid was then digested for 15 min at 50 °C with DpnI (Fermentas). The circular DNA was PCR-amplified after addition of a ColE1 reverse-strand primer to the digested mixture. The amplified products were treated with DpnI for 3 h at 37 °C and transfected into DH10β cells (Invitrogen) by electroporation.

The *E. coli* strains BL21(DE3) (Stratagene) and Acella (Edge Biosystems) were used for expression of all recombinant proteins. Bacteria were grown at 37 °C in LB or autoinduction⁴³ medium containing 50 mg l⁻¹ ampicillin. Media for expression of ClipZn2 were supplemented with 0.1 mM ZnCl₂. We induced protein expression in LB when cultures reached A₆₀₀ = 0.6–0.8 by adding IPTG to 1 mM and further incubating at 20 °C overnight. N-terminal His₆-tagged fusion proteins were affinity purified by immobilized metal-affinity chromatography on Ni²⁺-Sepharose (Amersham) at 4 °C according to the manufacturer's instructions. Buffers used for purification of ClipZn2 proteins contained 5 mM β-mercaptoethanol and 0.1 mM ZnCl₂.

For separation of the recombinant proteins from the N-terminal His₆ tag, proteins were dialyzed against thrombin cleavage buffer (20 mM Tris-HCl (pH 7.5), 150 mM NaCl, 2.5 mM CaCl₂). Proteolytic cleavage was carried out overnight at 4 °C using human thrombin (Sigma) at a concentration of 2.5 U per milligram of recombinant protein. Finally, all proteins were gel-filtered on a Superdex-75 column (Amersham) equilibrated in 20 mM Tris-HCl (pH 7.5) supplemented with 75 mM NaCl, except for the C-terminal CLIP170 fragments, which were run in the presence of an additional 5 mM β-mercaptoethanol and 0.1 mM ZnCl₂.

The homogeneity of the recombinant proteins was assessed by SDS-PAGE, and their identities were confirmed by mass spectral analyses and N-terminal sequencing. Tubulin was obtained from Cytoskeleton.

Biophysical studies. Static light-scattering and ITC experiments were done as described¹⁷. For static light-scattering analyses, 100 μl protein solution (3 mg ml⁻¹) was injected at a constant flow rate of 0.5 ml min⁻¹ onto a Superose 12 10/30 (Amersham Biosciences) size-exclusion column equilibrated in 20 mM Tris (pH 7.4) supplemented with 50 mM NaCl. The molecular masses were determined with Wyatt Astra version 4.90.08 (Wyatt Technology). ITC experiments were performed at 25 °C. The sample cell and syringe were filled with ~100 μM CLIP170 or EB1 (monomer equivalents) and ~1 mM p150n protein solution, respectively. The proteins had been extensively dialyzed against 10 mM sodium phosphate buffer (pH 7.4) supplemented with 150 mM NaCl before each experiment. Buffers for experiments carried out

with ClipZn fragments contained, in addition, 5 mM β-mercaptoethanol and 0.1 mM ZnCl₂. The binding isotherms were fit using a nonlinear least-squares minimization method provided with the VP-ITC calorimeter (MicroCal).

FRET experiments were done as described¹⁹. The internal FRET sensors were generated from YFP-CLIP170 (ref. 42) using a PCR-based strategy. In YFP-CLIP-BamHI-CFP-CLIP-C, the CFP surrounded by short glycine linkers was inserted after position 3902 of the cDNA corresponding to NCBI CoreNucleotide AJ237670; in YFP-CLIP-EcoRI-CFP-CLIP-C, the CFP surrounded by short glycine linkers was inserted after position 3755. These constructs were transfected into HEK293 cells with Lipofectamine 2000 (Invitrogen). One day later, cells were lysed in a buffer containing 20 mM Tris-HCl (pH 7.5), 100 mM NaCl, protease inhibitors (Complete, Roche), 1% (v/v) Triton X-100 and 10% (v/v) glycerol. The lysates were precleared by centrifugation at 16,000g for 20 min at 4 °C. For measurements of spectra, cell extracts were diluted 1:5 in PBS or in PME buffer (80 mM PIPES (pH 6.9), 1 mM MgCl₂, 1 mM EGTA) and incubated without or with the addition of 1–10 μM exogenous protein. Taxol-stabilized microtubules were prepared as described¹⁹. Emission spectra were measured using an F-4500 Hitachi fluorescence spectrophotometer with excitation at 425 nm (CFP). In cases where loss of sensitized YFP emission was observed, fluorescence spectra with excitation at 485 nm were measured to confirm that YFP was still intact. Spectra were not corrected for PME sensitivity. Background fluorescence of a crude extract prepared in the same way was negligible. The spectra shown in Figure 6b–d were scaled using the CFP emission peak at 475 nm as a reference to emphasize the changes in the profiles observed in different experiments.

Crystal structure determination. Crystals were grown at 20 °C in sitting drops. We mixed p150n and ClipZn2 protein solutions (2 mM each) in a 1:1 ratio and incubated for 30 min at room temperature before setting up the crystallization drops. Crystals grew within 3–5 d in the presence of 1.2 M trisodium citrate and 0.1 M HEPES (pH 7.0). Synchrotron data sets were collected at the Swiss Light Source protein beam line X06SA on a MAR CCD detector. All X-ray diffraction data were collected at 100 °K. Data collection and refinement

Table 2 Data collection and refinement statistics

	p150n–ClipZn2
Data collection	
Space group	C222 ₁
Cell dimensions	
<i>a</i> , <i>b</i> , <i>c</i> (Å)	116.1, 116.2, 79.9
Resolution (Å)	50 (2.6)
<i>R</i> _{sym}	14.1 (50.2)
<i>I</i> / σ <i>I</i>	11.6 (4.3)
Completeness (%)	99.5 (100.0)
Redundancy	6.571 (6.503)
Refinement	
Resolution (Å)	2.6
No. reflections	111,062
<i>R</i> _{work} / <i>R</i> _{free}	0.27 / 0.33
No. atoms	
Protein	2,965
Ions	4
Water	51
<i>B</i> -factors	
Protein	29.8
Ions	27.6
Water	17.5
R.m.s. deviations	
Bond lengths (Å)	0.013
Bond angles (°)	1.4

X-ray diffraction data were collected from one crystal. Values in parentheses are for highest-resolution shell.

statistics are summarized in **Table 2**. The structure was solved by molecular replacement using MOLREP⁴⁴. Search models were based on the structure of p150n (PDB 2HKN). Residues Pro26–Phe97 of p150n and Pro1406–Phe1427 of ClipZn2 are visible in the crystal structure. Of these residues, 84.4% fall in the most favored region of the Ramachandran plot, and 15.3% and 0.3% are in the additionally and generously allowed regions, respectively. The refined model of the p150n–ClipZn2 complex has R -factors of 27% and 33% for R_{work} and R_{free} , respectively. We were not surprised by these relatively high values, considering that >30% of all residues are disordered and do not yield interpretable electron densities. The quality of the model is underscored by the very high similarity (r.m.s. deviation for all atoms equals 0.47 Å) to the p150n–ClipZn2 structure solved at 1.8-Å resolution in the accompanying study³⁹, which has R -factors of 19.4% and 21.6% for R_{work} and R_{free} , respectively. Figures were prepared with PyMOL (<http://pymol.sourceforge.net>).

Fluorescence microscopy. COS-7 cells were transfected with CLIP170 fusion constructs using FuGENE 6 (Roche). One day later, cells were fixed and stained as described¹⁹. Mouse monoclonal antibodies raised against p150^{Glued} (BD Biosciences) and Alexa 594-conjugated goat anti-mouse (Invitrogen) were used for staining. Samples were analyzed with a Leica DMRBE microscope equipped with a PL Fluotar ×100 1.3 NA objective, FITC/EGFP filter 41012 (Chroma) and Texas Red filter 41004 (Chroma) and an ORCA-ER-1394 CCD camera C4742-80-12AG (Hamamatsu). We projected 16-bit images onto the CCD chip at a magnification of 0.1 μm pixel⁻¹. Images were converted to 8 bits and prepared for publication using Adobe Photoshop.

Accession codes. Protein Data Bank: Coordinates have been deposited with accession code 2PZO.

Note: Supplementary information is available on the Nature Structural & Molecular Biology website.

ACKNOWLEDGMENTS

We thank I. Hayashi for providing data before publication, F. Winkler and D. Kostrewa for support with the X-ray data processing, T. Güntert and Y. Bächtiger for technical assistance and C. Weirich for careful reading of the manuscript. X-ray data were collected at beamline X06SA of the Swiss Light Source. This work was supported by the Swiss National Science Foundation through grant 3100A0-109423 (to M.O.S.) and within the framework of the National Center of Competence in Research Structural Biology program.

AUTHOR CONTRIBUTIONS

A.W. and S.H. designed and executed the cloning, protein purification and structure determination. R.J. designed and executed the cloning. O.O. and I.J. designed and executed the ITC experiments. D.F. purified the protein. A.A. designed and executed the fluorescence microscopy and FRET experiments and wrote the paper. M.O.S. designed the research, guided the project and wrote the paper.

Published online at <http://www.nature.com/nsmb>

Reprints and permissions information is available online at <http://npg.nature.com/reprintsandpermissions>

- Riehemann, K. & Sorg, C. Sequence homologies between four cytoskeleton-associated proteins. *Trends Biochem. Sci.* **18**, 82–83 (1993).
- Gundersen, G.G. Evolutionary conservation of microtubule-capture mechanisms. *Nat. Rev. Mol. Cell Biol.* **3**, 296–304 (2002).
- Galjart, N. & Perez, F. A plus-end raft to control microtubule dynamics and function. *Curr. Opin. Cell Biol.* **15**, 48–53 (2003).
- Carvalho, P., Tirnauer, J.S. & Pellman, D. Surfing on microtubule ends. *Trends Cell Biol.* **13**, 229–237 (2003).
- Howard, J. & Hyman, A.A. Dynamics and mechanics of the microtubule plus end. *Nature* **422**, 753–758 (2003).
- Vaughan, K.T. Surfing, regulating and capturing: are all microtubule-tip-tracking proteins created equal? *Trends Cell Biol.* **14**, 491–496 (2004).
- Galjart, N. CLIPs and CLASPs and cellular dynamics. *Nat. Rev. Mol. Cell Biol.* **6**, 487–498 (2005).
- Akhmanova, A. & Hoogenraad, C.C. Microtubule plus-end-tracking proteins: mechanisms and functions. *Curr. Opin. Cell Biol.* **17**, 47–54 (2005).
- Miller, R.K., D'Silva, S., Moore, J.K. & Goodson, H.V. The CLIP-170 orthologue Bik1p and positioning the mitotic spindle in yeast. *Curr. Top. Dev. Biol.* **76**, 49–87 (2006).
- Badin-Larcon, A.C. *et al.* Suppression of nuclear oscillations in *Saccharomyces cerevisiae* expressing Glu tubulin. *Proc. Natl. Acad. Sci. USA* **101**, 5577–5582 (2004).
- Wen, Y. *et al.* EB1 and APC bind to mDia to stabilize microtubules downstream of Rho and promote cell migration. *Nat. Cell Biol.* **6**, 820–830 (2004).
- Erck, C. *et al.* A vital role of tubulin-tyrosine-ligase for neuronal organization. *Proc. Natl. Acad. Sci. USA* **102**, 7853–7858 (2005).
- Peris, L. *et al.* Tubulin tyrosination is a major factor affecting the recruitment of CAP-Gly proteins at microtubule plus ends. *J. Cell Biol.* **174**, 839–849 (2006).
- Li, S. *et al.* Crystal structure of the cytoskeleton-associated protein glycine-rich (CAP-Gly) domain. *J. Biol. Chem.* **277**, 48596–48601 (2002).
- Saito, K. *et al.* The CAP-Gly domain of CYLD associates with the proline-rich sequence in NEMO/IKK γ . *Structure* **12**, 1719–1728 (2004).
- Hayashi, I., Wilde, A., Mal, T.K. & Ikura, M. Structural basis for the activation of microtubule assembly by the EB1 and p150^{Glued} complex. *Mol. Cell* **19**, 449–460 (2005).
- Honnappa, S. *et al.* Key interaction modes of dynamic +TIP networks. *Mol. Cell* **23**, 663–671 (2006).
- Goodson, H.V. *et al.* CLIP-170 interacts with dynactin complex and the APC-binding protein EB1 by different mechanisms. *Cell Motil. Cytoskeleton* **55**, 156–173 (2003).
- Lansbergen, G. *et al.* Conformational changes in CLIP-170 regulate its binding to microtubules and dynactin localization. *J. Cell Biol.* **166**, 1003–1014 (2004).
- Ligon, L.A., Shelly, S.S., Tokito, M.K. & Holzbaur, E.L. Microtubule binding proteins CLIP-170, EB1, and p150^{Glued} form distinct plus-end complexes. *FEBS Lett.* **580**, 1327–1332 (2006).
- Sheeman, B. *et al.* Determinants of *S. cerevisiae* dynein localization and activation: implications for the mechanism of spindle positioning. *Curr. Biol.* **13**, 364–372 (2003).
- Watson, P. & Stephens, D.J. Microtubule plus-end loading of p150^{Glued} is mediated by EB1 and CLIP-170 but is not required for intracellular membrane traffic in mammalian cells. *J. Cell Sci.* **119**, 2758–2767 (2006).
- Dujardin, D. *et al.* Evidence for a role of CLIP-170 in the establishment of metaphase chromosome alignment. *J. Cell Biol.* **141**, 849–862 (1998).
- Puls, I. *et al.* Mutant dynactin in motor neuron disease. *Nat. Genet.* **33**, 455–456 (2003).
- Levy, J.R. *et al.* A motor neuron disease-associated mutation in p150^{Glued} perturbs dynactin function and induces protein aggregation. *J. Cell Biol.* **172**, 733–745 (2006).
- Krishna, S.S., Majumdar, I. & Grishin, N.V. Structural classification of zinc fingers: survey and summary. *Nucleic Acids Res.* **31**, 532–550 (2003).
- Honnappa, S., John, C.M., Kostrewa, D., Winkler, F.K. & Steinmetz, M.O. Structural insights into the EB1-APC interaction. *EMBO J.* **24**, 261–269 (2005).
- Askham, J.M., Vaughan, K.T., Goodson, H.V. & Morrison, E.E. Evidence that an interaction between EB1 and p150^{Glued} is required for the formation and maintenance of a radial microtubule array anchored at the centrosome. *Mol. Biol. Cell* **13**, 3627–3645 (2002).
- Yan, X., Habedanck, R. & Nigg, E.A. A complex of two centrosomal proteins, CAP350 and FOP, cooperates with EB1 in microtubule anchoring. *Mol. Biol. Cell* **17**, 634–644 (2006).
- Parvari, R. *et al.* Mutation of TBCE causes hypoparathyroidism-retardation-dysmorphism and autosomal recessive Kenny-Caffey syndrome. *Nat. Genet.* **32**, 448–452 (2002).
- Folker, E.S., Baker, B.M. & Goodson, H.V. Interactions between CLIP-170, tubulin, and microtubules: implications for the mechanism of Clip-170 plus-end tracking behavior. *Mol. Biol. Cell* **16**, 5373–5384 (2005).
- Tirnauer, J.S., Grego, S., Salmon, E.D. & Mitchison, T.J. EB1-microtubule interactions in *Xenopus* egg extracts: role of EB1 in microtubule stabilization and mechanisms of targeting to microtubules. *Mol. Biol. Cell* **13**, 3614–3626 (2002).
- Vaughan, P.S., Miura, P., Henderson, M., Byrne, B. & Vaughan, K.T. A role for regulated binding of p150^{Glued} to microtubule plus ends in organelle transport. *J. Cell Biol.* **158**, 305–319 (2002).
- Karki, S. & Holzbaur, E.L. Cytoplasmic dynein and dynactin in cell division and intracellular transport. *Curr. Opin. Cell Biol.* **11**, 45–53 (1999).
- Allan, V. Dynactin. *Curr. Biol.* **10**, R432 (2000).
- Busch, K.E., Hayles, J., Nurse, P. & Brunner, D. Tea2p kinesin is involved in spatial microtubule organization by transporting tip1p on microtubules. *Dev. Cell* **6**, 831–843 (2004).
- Busch, K.E. & Brunner, D. The microtubule plus end-tracking proteins mal3p and tip1p cooperate for cell-end targeting of interphase microtubules. *Curr. Biol.* **14**, 548–559 (2004).
- Perez, F., Diamantopoulos, G.S., Stalder, R. & Kreis, T.E. CLIP-170 highlights growing microtubule ends *in vivo*. *Cell* **96**, 517–527 (1999).
- Hayashi, I., Plevin, M.J. & Ikura, M. Activation of microtubule assembly by plus-end tracking proteins: regulatory interplays between EB1, CLIP-170 and p150^{Glued}. *Nat. Struct. Mol. Biol.*, advance online publication 9 September 2007 (doi:10.1038/nsmb1299).
- Westermann, S. & Weber, K. Post-translational modifications regulate microtubule function. *Nat. Rev. Mol. Cell Biol.* **4**, 938–947 (2003).
- Scheel, J. *et al.* Purification and analysis of authentic CLIP-170 and recombinant fragments. *J. Biol. Chem.* **274**, 25883–25891 (1999).
- Komarova, Y. *et al.* EB1 and EB3 control CLIP dissociation from the ends of growing microtubules. *Mol. Biol. Cell* **16**, 5334–5345 (2005).
- Studier, F.W. Protein production by auto-induction in high density shaking cultures. *Protein Expr. Purif.* **41**, 207–234 (2005).
- Collaborative Computational Project, Number 4. The CCP4 suite: programs for protein crystallography. *Acta Crystallogr. D Biol. Crystallogr.* **50**, 760–763 (1994).